2014 IEEE International Conference on Robotics & Automation (ICRA)
Hong Kong Convention and Exhibition Center
May 31 - June 7, 2014. Hong Kong, China

Revisiting Coverage Control in Nonconvex Environments using Visibility Sets*

Lukas Klodt, Dominik Haumann and Volker Willert

Abstract— **In the context of robotics coverage describes the deployment of mobile sensors or agents in a target area. This paper presents a new solution to coverage in nonconvex environments. We apply a modification to the coverage approach in [1], making use of visibility sets and a contraction of the environment, leading to a change in the bounds of integration. The resulting feedback control is fully distributed, has guaranteed, inherent collision avoidance without separate path planning and reduced communication and computation requirements compared to similar approaches. We also formulate an extension to agents with limited sensing range. Our method works in unknown environments, if all regions are of equal interest. We provide simulation results demonstrating the advantageous properties of the approach.**

I. INTRODUCTION

The motion coordination of groups of autonomous vehicles, mobile sensors or multi-robot systems is a challenging and prevalent topic in the robotics community. The technologic advancement of sensor nodes with mobility and networking capabilities opens up new application possibilities. In most cases an important aspect is the distributed structure of such systems, i.e., there is no centralized processing station to coordinate the agents[1]. Instead, the mobile sensors have to act autonomously relying only on local information to find a good solution to a common task [2]. This leads to independence of a basis station and higher robustness towards failing agents.

A. Introduction to Coverage

The considered task in this case is the optimal deployment of mobile sensors in an environment: The sensors are placed at possibly random locations in the target area and have to spread out to reach a stable arrangement. Possible applications include distributed measurement, surveillance or search and rescue missions.

A popular solution to this problem was presented in [1] and is referred to as *coverage control* or *Voronoi coverage*. The authors formulate the task as a geometric optimization problem. This kind of resource allocation task was already investigated in the context of information theory and vector quantization [3] and for facility location problems [4] (e.g., where to place radio stations to cover an area as good as possible). The resulting solution is a continuous-time version of the Lloyd algorithm [3], which consists of the following steps:

- Compute the Voronoi partition of the environment using sensor positions as generators.
- Move all sensors towards the centroids of their respective Voronoi cells.
- Repeat until convergence is achieved.

This algorithm is formulated as a feedback control law that allows distributed, adaptive and asynchronous minimization of the optimization function. A lot of extensions to this approach have been developed including: range limitations [5], utilization of anisotropic sensors [6] and estimation of importance of different areas [7]. The coverage framework has also been modified to fulfill different tasks like target tracking [8] and multi-robot exploration [9].

B. Literature on Coverage in Nonconvex Environments

The main drawback of Voronoi coverage is that it only works in convex environments, which is a strong limitation since real world environments are usually nonconvex. The arising complications are already discussed in [10] with several examples and can be summarized to two cases: The centroid lies inside the environment but the trajectory crosses through impassable regions, or the centroid lies outside the environment. In both cases the robots would collide with the environment and the final configuration is not clearly defined in the second case. These issues have been addressed in several different ways in the literature. The existing approaches are summarized in the following.

In [11], among other extensions, Voronoi coverage is applied to simple polygons without holes using the generalized gradient of the geodesic distance. The authors of [12] propose a transformation for a class of nonconvex environments that allows the application of the coverage algorithm. Mapping back to the original domain gives the solution to the problem. The geometry and a suitable diffeomorphism are assumed to be known beforehand. For a convex set with obstacles the approach converges to the solution of the original problem if it belongs to the interior [13], but in other cases the solution can be suboptimal. Breitenmoser et al. [10] show that for general nonconvex environments a path planning procedure or obstacle avoidance is necessary. They combine the Lloyd algorithm for target point calculation with a local path planner and prove the convergence of the proposed control strategy. The path planner constrains outlying target points to the environment using a projection procedure. A combination of Voronoi coverage and a

*This work was supported by the German Research Foundation (DFG) within the GRK 1362.

All authors are with the Institute of Automatic Control and Mechatronics, Technische Universität Darmstadt, Landgraf-Georg-Str. 4, 64283 Darmstadt, Germany {lklodt, dhaumann, vwillert}@rtr.tu-darmstadt.de

[1]The terms sensor, robot and agent are used interchangeably and refer to an entity which has computation, sensing, communication and locomotion capabilities.

978-1-4799-3684-7/14/$31.00 ©2014 IEEE

potential field method is presented in [14]. The approach is a direct extension to the potential field method from [15], adding an additional attractive potential towards the centroid of each robots Voronoi cell. The authors show that their approach yields better final configurations than [15] in selected examples, but do not specify the case where a centroid lies inside an obstacle and provide no theoretical results towards convergence. In [16], Durham et al. propose a coverage strategy on a discretized environment represented by a graph. They define the generalized centroid as the point inside a connected subset that minimizes the sum of weighted distances to all other points. Due to the discretization this point can be found with an exhaustive search or an appropriate heuristic. The authors provide convergence proofs under reduced communication requirements, i.e., only pairwise communication is necessary.

The usage and maximization of visibility sets has been studied extensively in the context of the *art gallery problem*. Solutions to a distributed version of the art gallery problem with mobile sensors have been developed and proven in [17], [18]. The optimization goal is different compared to Voronoi coverage even though it overlaps in some cases.

Also related to our work is the problem presented in [19]. The authors consider a modified coverage framework where overlapping sensor areas increase the quality of coverage and the environment with polygonal obstacles is no longer partitioned into Voronoi cells. The common ground lies in the approach that obstacles attenuate or block the sensing abilities of the robots, leading to a closer analysis of the gradient of the optimization function. The authors show that the use of a generalized gradient is necessary due to a new term that arises from the frontiers to invisible regions.

The combination of Voronoi coverage and limited visibility has only been considered recently by [20] and [21]. In [20] a visibility-based Voronoi diagram is introduced and the authors propose a projection of the centroid to the closest point inside the visible Voronoi cell. A second algorithm considers frontiers to invisible regions, towards which the robots are directed to uncover new areas. The authors provide simulations but no theoretical guarantees that the robots stay inside the environment and converge to a stable configuration. Marier et al. [21] also use the notion of a visible Voronoi diagram similar to [20] with the difference that they allow disconnected cells. The gradient of the optimization function is analyzed leading to similar results as in [19]. A proof of convergence is given for environments without holes. The problem that agents might leave the environment is again handled by a projection procedure.

C. Contribution of this paper

One of the main drawbacks of existing approaches is that they have to rely on separate path planning or projection procedures to ensure collision avoidance with the boundary of the environment and obstacles. Additionally in some cases they only work for certain types of environments.

We present a new approach based on [1] that consists of a virtual growing of the environment and the use of visibility sets. The resulting coverage strategy has inherent collision avoidance properties without the use of explicit path planning, obstacle avoidance behavior or projections into the allowable area and works in arbitrary nonconvex environments. Additionally, our method has lower requirements on communication and computation capabilities compared to similar solutions. The advantageous properties of Voronoi coverage are retained, i.e., the solution is distributed and the agents can adapt to failing or new sensor nodes or changing density functions. Furthermore, while we assume vehicles with single integrator dynamics, the method can be extended to other system dynamics following [22].

The next section begins with an introduction to notations we use and the problem formulation, including the description of the coverage approach for convex environments. Section III contains our extension to nonconvex domains for unlimited as well as limited sensing range. Simulation results and a discussion are presented in Section IV. The last section completes this paper with a conclusion and an outlook on future research.

II. PROBLEM STATEMENT

A. Preliminaries

Although the problem can be formulated in higher dimensions, we limit our considerations to planar environments $\mathcal{Q} \subset \mathbb{R}^2$ for ease of notation. The boundary and the interior of a set $\mathcal{Q}$ are written as $\partial\mathcal{Q}$ and $\text{int}(\mathcal{Q})$, respectively. The collection of all sensor positions $\boldsymbol{p}_i \in \mathcal{Q}$ is called configuration and aggregated in the $2N$-dimensional vector $\boldsymbol{P} = [\boldsymbol{p}_1^\mathsf{T}, \dots, \boldsymbol{p}_N^\mathsf{T}]^\mathsf{T}$. Define the set of all points closer to $\boldsymbol{p}_i$ than to all other robots as Voronoi cell $\mathcal{V}_i = \{\boldsymbol{q} \in \mathcal{Q} \mid \|\boldsymbol{q} - \boldsymbol{p}_i\| \leq \|\boldsymbol{q} - \boldsymbol{p}_j\|, \forall j \neq i\}$ and let $\mathcal{V} = \{\mathcal{V}_1, \dots, \mathcal{V}_N\}$ be the Voronoi partition, with $\|\cdot\|$ denoting the Euclidean distance. According to this definition, the union of all cells is $\mathcal{Q}$ and the interiors of any two distinct cells share no common points. We refer to robots with adjoining Voronoi cells as neighbors and assume ideal, bidirectional communication between neighbors. The graph consisting of all edges between Voronoi neighbors is called Delaunay graph and is dual to the Voronoi diagram. As in most other related work we assume agents have omnidirectional vision and can locate in a common coordinate frame.

B. Coverage Control

Voronoi coverage as presented in [1] originates from the minimization of an objective function, dependent on the configuration $\boldsymbol{P}$ and a partition of the environment into dominance regions assigned to each sensor. The authors show that the optimal partition for the proposed setting is the Voronoi diagram, using the positions $\boldsymbol{p}_i$ as generators in the way described above. This simplifies the optimization in that the objective function now only depends on the configuration:

$$H(\boldsymbol{P}) = \sum_{i=1}^{N} \int_{\mathcal{V}_i} f(\|\boldsymbol{q} - \boldsymbol{p}_i\|)\phi(\boldsymbol{q})d\boldsymbol{q}. \tag{1}$$

Therein, $f : \mathbb{R}_{\geq 0} \to \mathbb{R}_{\geq 0}$ denotes a nondecreasing performance function that characterizes degrading sensing performance with increasing distance. Further, the density function $\phi : \mathcal{Q} \to \mathbb{R}_{\geq 0}$ encodes a location dependent measure of information or probability that an event takes place. The argument of f can be a more general distance function, but we will keep the Euclidean distance for the following.

According to [1], the necessary condition for $H(\boldsymbol{P})$ to be minimized is

$$\frac{\partial H(\boldsymbol{P})}{\partial \boldsymbol{p}_i} = \int_{\mathcal{V}_i} \frac{\partial}{\partial \boldsymbol{p}_i} f(\|\boldsymbol{q} - \boldsymbol{p}_i\|)\phi(\boldsymbol{q})d\boldsymbol{q} = \boldsymbol{0}, \qquad (2)$$

and using $f(x) = x^2$ provides

$$\frac{\partial H(\boldsymbol{P})}{\partial \boldsymbol{p}_i} = \int_{\mathcal{V}_i} -2(\boldsymbol{q} - \boldsymbol{p}_i)\phi(\boldsymbol{q})d\boldsymbol{q} = -2A_i(\boldsymbol{c}_i - \boldsymbol{p}_i), \quad (3)$$

where $A_i = \int_{\mathcal{V}_i} \phi(\boldsymbol{q})d\boldsymbol{q}$ is the ϕ-weighted area of $\mathcal{V}_i$ and $\boldsymbol{c}_i = A_i^{-1} \int_{\mathcal{V}_i} \boldsymbol{q}\phi(\boldsymbol{q})d\boldsymbol{q}$ is the center of mass or centroid of the region. The control law for simple first order dynamics $\dot{\boldsymbol{p}}_i = \boldsymbol{u}_i$ can be set to

$$\boldsymbol{u}_i = k(\boldsymbol{c}_i - \boldsymbol{p}_i) \propto -\frac{\partial H(\boldsymbol{P})}{\partial \boldsymbol{p}_i} \qquad (4)$$

with a positive gain k. In a convex environment all Voronoi cells are convex [1] and therefore the centroid always lies inside the corresponding cell. The solution converges to a local minimum where the sensor positions coincide with the centroids of their respective Voronoi cells and the resulting partition is called centroidal Voronoi tesselation. The partial derivative is distributed in the sense that each robot only requires the location of its neighbors in the Delaunay graph to compute the control input.

As suggested in the introduction the problem is now that we want to transfer Voronoi coverage to nonconvex environments.

Problem. Find a distributed control law based on distributed optimization similar to (4) and (1) such that all $\boldsymbol{p}_i$ stay inside a nonconvex environment $\mathcal{Q}$ for all t and converge to a stable configuration.

III. NONCONVEX COVERAGE

For all further considerations the environment is defined by a simple[2] polygon $\mathcal{B}$ and the set of simple polygonal obstacles $\mathcal{O}_1, \ldots, \mathcal{O}_m \subset \mathcal{B}$. The maneuverable domain for the mobile sensors is consequently $\mathcal{Q} := \mathcal{B} \setminus \cup_{i=1}^m \mathcal{O}_i$. A vertex of $\mathcal{Q}$ is convex, if its interior angle is less than or equal to π radians, otherwise the vertex is concave.

The main aspect of our contribution consists of a combination of two modifications to the original problem in (1). In conjunction with an approximation of the gradient, the proposed approach leads to the desired behavior. The two modifications are 1) the use of visibility sets and 2) the application of a δ-contraction to the environment.

[2]A simple polygon is non-self-intersecting and contains no holes.

A. *Visibility*

First, let us consider the notion of visibility. Given a set $\mathcal{Q} \subset \mathbb{R}^2$ and a point $\boldsymbol{p}_i \in \mathcal{Q}$. A point $\boldsymbol{q} \in \mathcal{Q}$ is visible from $\boldsymbol{p}_i$ if the closed path segment $[\boldsymbol{p}_i, \boldsymbol{q}] = \{\boldsymbol{p}_i + \lambda(\boldsymbol{q} - \boldsymbol{p}_i) \mid \lambda \in [0, 1]\}$ is contained in $\mathcal{Q}$, i.e., $[\boldsymbol{p}_i, \boldsymbol{q}] \subset \mathcal{Q}$. The set of all points $\boldsymbol{q} \in \mathcal{Q}$ visible from $\boldsymbol{p}_i$ is the visibility set with respect to $\boldsymbol{p}_i$, denoted as $\mathcal{S}^\star(\boldsymbol{p}_i)$. The visibility set is a star-shaped domain and represents exactly the parts of the environment that are visible from a robot location.

There are several reasons to use visibility sets in this context. The first one is the realistic consideration that sensing capability may be attenuated or completely blocked by obstacles. Using solely the Euclidean distance to characterize sensing performance is no longer viable in the presence of obstacles. Second, the use of visibility allows coverage to be performed in unknown environments, assuming there are no regions with higher priority. Otherwise, knowledge of the density function is still necessary. The third reason is that the limited visibility actually helps to provide a guarantee that the robot stays inside the environment.

Following these thoughts it makes sense to define a new Voronoi partition tailored to our visibility-limited setting. One option is the usage of the geodesic distance as in [11] and limiting the geodesic Voronoi cells to the visibility set. Another option is the definition proposed in [20] and [21], allowing points closer to one robot to be assigned to another if they are invisible to the former.

Instead, we propose the use of a simpler, visibility-limited Voronoi cell (VLVC)

$$\mathcal{V}_i^\star = \{\boldsymbol{q} \in \mathcal{S}^\star(\boldsymbol{p}_i) \mid \|\boldsymbol{q} - \boldsymbol{p}_i\| \leq \|\boldsymbol{q} - \boldsymbol{p}_j\|, \forall j \neq i\}. \quad (5)$$

Accordingly, the visibility-limited Voronoi diagram is the set $\mathcal{V}^\star = \{\mathcal{V}_1^\star, \ldots, \mathcal{V}_N^\star\}$. This definition can be seen as a simple intersection between the Voronoi cell and the visibility set of each robot. Some regions that might be visible are disregarded and treated as invisible, but the computation and communication requirements are reduced compared to other definitions (cf. Section IV-B). Range requirements for communication remain the same as in convex environments, i.e., communication is necessary between neighbors in $\mathcal{V}$.

Note that $\mathcal{V}^\star$ is no longer always a partition of $\mathcal{Q}$ since $\cup_{i=1}^N \mathcal{V}_i^\star \subseteq \mathcal{Q}$. The set of invisible points is $\mathcal{Q}_0 = \mathcal{Q} \setminus \cup_{i=1}^N \mathcal{V}_i^\star$.

B. *δ-contraction*

The second modification, as mentioned above, is the application of a δ-contraction, also known as growing of obstacles in robotics for collision-free path planning [23]. For an environment $\mathcal{Q}$, the δ-contraction is defined as $\mathcal{Q}_\delta = \{\boldsymbol{q} \in \mathcal{Q} \mid \inf_{\boldsymbol{q}' \in \partial\mathcal{Q}} \|\boldsymbol{q} - \boldsymbol{q}'\| \geq \delta\}$, i.e., the set of all points in $\mathcal{Q}$ with a distance to the boundary of $\mathcal{Q}$ greater than or equal to δ (see Fig. 1).

A remarkable property of the δ-contraction is the following: For arbitrary small $\delta > 0$ the boundary $\partial\mathcal{Q}_\delta$ of the δ-contraction is continuously differentiable in all $\boldsymbol{q} \in \partial\mathcal{Q}_\delta$ except in the convex vertices. All concave vertices grow by δ, yielding a differentiable circular segment.

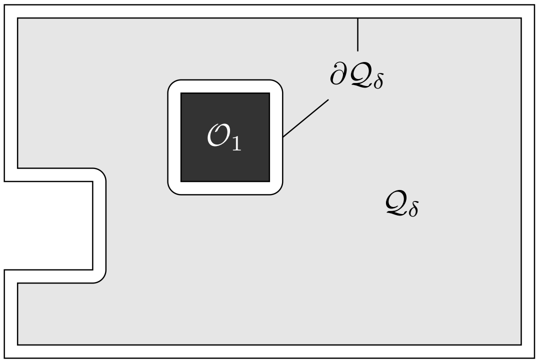

Fig. 1: Environment $\mathcal{Q}$ and the corresponding δ-contraction

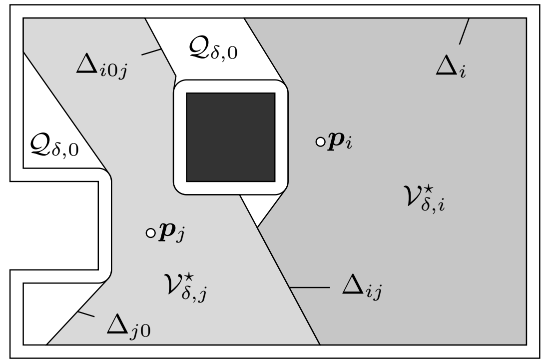

Fig. 2: Different types of frontiers

Depending on the environment and the value of δ, a connected set $\mathcal{Q}$ can have a disconnected $\mathcal{Q}_\delta$. However, considering the previous remark, if $\mathcal{Q}$ is connected, δ can always be selected in a way that $\mathcal{Q}_\delta$ is also connected.

C. Derivation of the Objective Function

Given a nonconvex environment $\mathcal{Q}$ as defined in the beginning of this section, we propose to apply Voronoi coverage to the δ-contraction of the environment in a limited visibility setting. For this purpose we define the performance function

$$f_{\text{vis}}(\|\boldsymbol{q}-\boldsymbol{p}_i\|) = \begin{cases} \|\boldsymbol{q}-\boldsymbol{p}_i\|^2, & \text{if } \boldsymbol{q} \in \cup_{j=1}^N \mathcal{V}_j^\star \\ D^2, & \text{if } \boldsymbol{q} \in \mathcal{Q}_0 \end{cases} \tag{6}$$

with D being a parameter that penalizes invisible areas and controls the uncovering of such regions. Note that f_{vis} is completely defined on $\mathcal{Q}$ since $(\cup_{j=1}^N \mathcal{V}_j^\star) \cup \mathcal{Q}_0 = \mathcal{Q}$, with discontinuities at the frontiers to invisible regions that will be specified in the upcoming paragraphs.

Now, applying the δ-contraction to $\mathcal{Q}$, the resulting objective function on the domain $\mathcal{Q}_\delta$ is

$$H_{\text{vis}}(\boldsymbol{P}) = \sum_{i=1}^N \int_{\mathcal{V}^\star_{\delta,i}} \|\boldsymbol{q}-\boldsymbol{p}_i\|^2 \phi(\boldsymbol{q}) d\boldsymbol{q} + \int_{\mathcal{Q}_{\delta,0}} D^2 \phi(\boldsymbol{q}) d\boldsymbol{q}, \tag{7}$$

with $\mathcal{V}^\star_{\delta,i} = \{\boldsymbol{q} \in \mathcal{V}_i^\star \mid [\boldsymbol{p}_i, \boldsymbol{q}] \subset \mathcal{Q}_\delta\}$ denoting the VLVC and $\mathcal{Q}_{\delta,0} = \mathcal{Q}_\delta \setminus \cup_{i=1}^N \mathcal{V}^\star_{\delta,i}$ denoting the invisible area, both in the new shrunken environment $\mathcal{Q}_\delta$. Unfortunately, the partial derivative of H_{vis} is more complicated compared to (2). For a better understanding of the derivations, we consider the coordinates of $\boldsymbol{p}_i = [x_i, y_i]^\mathsf{T}$ separately.

Remark 1: Similar to [19], we initially assume that $\boldsymbol{p}_i$ is not on a polygonal inflection or bitangent, where $H_{\text{vis}}(\boldsymbol{P})$ is not differentiable.

Using an extended form of the Leibniz integral rule for differentiation under the integral sign [24], as the domain of integration is a function of $\boldsymbol{P}$, gives

$$\frac{\partial H_{\text{vis}}(\boldsymbol{P})}{\partial x_i} = \sum_{j=1}^N \int_{\mathcal{V}^\star_{\delta,j}} \frac{\partial}{\partial x_i} \|\boldsymbol{q}-\boldsymbol{p}_j\|^2 \phi(\boldsymbol{q}) d\boldsymbol{q} \tag{8a}$$

$$+ \sum_{j=1}^N \int_{\partial\mathcal{V}^\star_{\delta,j}} \|\boldsymbol{q}-\boldsymbol{p}_j\|^2 \phi(\boldsymbol{q}) \boldsymbol{v}_j^\mathsf{T} \boldsymbol{n}_j ds \tag{8b}$$

$$+ \int_{\mathcal{Q}_{\delta,0}} \frac{\partial}{\partial x_i} D^2 \phi(\boldsymbol{q}) d\boldsymbol{q} \tag{8c}$$

$$+ \int_{\partial\mathcal{Q}_{\delta,0}} D^2 \phi(\boldsymbol{q}) \boldsymbol{v}_0^\mathsf{T} \boldsymbol{n}_0 ds, \tag{8d}$$

where $\boldsymbol{v}_j = \frac{\partial \boldsymbol{q}(\partial\mathcal{V}^\star_{\delta,j})}{\partial x_i}$ and $\boldsymbol{v}_0 = \frac{\partial \boldsymbol{q}(\partial\mathcal{Q}_{\delta,0})}{\partial x_i}$ are the derivatives of boundary points $\boldsymbol{q} \in \partial\mathcal{V}^\star_{\delta,j}$ and $\boldsymbol{q} \in \partial\mathcal{Q}_{\delta,0}$ with respect to x_i, interpreted as velocities of the moving boundaries. Further, $\boldsymbol{n}_j$ and $\boldsymbol{n}_0$ are the outward facing unit normals on the respective boundaries and ds is the element of arc length. Clearly, all elements of the sum in (8a) for $j \neq i$ and the term (8c) are zero, leaving only the integral over the i-th VLVC and the boundary terms (8b), (8d).

Taking a closer look at the boundary of a cell $\mathcal{V}^\star_{\delta,j}$, there are four different parts to distinguish (see also Fig. 2):

1) Boundary points on intersections with $\partial\mathcal{Q}_\delta$, denoted with $\Delta_j = \partial\mathcal{V}^\star_{\delta,j} \cap \partial\mathcal{Q}_\delta$, have a vanishing derivative $\frac{\partial \boldsymbol{q}(\Delta_j)}{\partial x_i} = 0$ for all j in static environments.
2) Boundary points on intersections with neighboring VLVC, denoted with $\Delta_{ij} = \Delta_{ji} = \partial\mathcal{V}^\star_{\delta,i} \cap \partial\mathcal{V}^\star_{\delta,j}$, have nonzero derivatives with respect to x_i in two cases, either $j = i$ or $j \in \mathcal{N}_i$, where $\mathcal{N}_i = \{j \in \{1, \ldots, N\} \mid \Delta_{ij} \neq \emptyset, j \neq i\}$ is the neighborhood of $\boldsymbol{p}_i$. The integrand of (8b) is identical in both cases, due to the definition of the VLVCs, with the exception that the outward normals point in opposite directions. This leads to

$$\int_{\partial\mathcal{V}^\star_{\delta,i} \setminus \partial\mathcal{Q}_{\delta,0}} \|\boldsymbol{q}-\boldsymbol{p}_i\|^2 \phi(\boldsymbol{q}) \boldsymbol{v}_i^\mathsf{T} \boldsymbol{n}_i ds$$

$$= -\sum_{j \in \mathcal{N}_i} \int_{\Delta_{ij}} \|\boldsymbol{q}-\boldsymbol{p}_j\|^2 \phi(\boldsymbol{q}) \boldsymbol{v}_j^\mathsf{T} \boldsymbol{n}_j ds$$

and elimination of the corresponding parts of the sum of integrals in (8b).

3) The third and remaining part on the boundary of a VLVC is the intersection with the boundary of the invisible area $\partial\mathcal{Q}_{\delta,0}$, denoted with $\Delta_{j0} = \partial\mathcal{V}^\star_{\delta,j} \cap \partial\mathcal{Q}_{\delta,0}$. Those parts result in nonzero terms out of (8b) and (8d) for $j = i$, and in the case explained in 4).
4) In some cases, the boundary of the Euclidean Voronoi cell $\mathcal{V}_i$ intersects with the boundary between the invisible area and another VLVC, e.g., the part that is labeled with $\Delta_{i0j} = \partial\mathcal{V}_i \cap \partial\mathcal{Q}_{\delta,0} \cap \mathcal{V}^\star_{\delta,j}$ in Fig. 2. This boundary will move with the position of $\boldsymbol{p}_i$, even though it is not part of the VLVC of robot i.

Concluding the above considerations, the remainder of (8) is reduced to

$$\frac{\partial H_{\text{vis}}(\boldsymbol{P})}{\partial x_i} = \int_{\mathcal{V}^\star_{\delta,i}} \frac{\partial}{\partial x_i}\|\boldsymbol{q}-\boldsymbol{p}_i\|^2\phi(\boldsymbol{q})d\boldsymbol{q} \tag{9a}$$

$$+\int_{\Delta_{i0}} (\|\boldsymbol{q}-\boldsymbol{p}_i\|^2 - D^2)\phi(\boldsymbol{q})\boldsymbol{v}_i^\mathsf{T}\boldsymbol{n}_i ds \tag{9b}$$

$$+\sum_{j\in\mathcal{M}_i}\int_{\Delta_{i0j}} (\|\boldsymbol{q}-\boldsymbol{p}_j\|^2 - D^2)\phi(\boldsymbol{q})\boldsymbol{v}_j^\mathsf{T}\boldsymbol{n}_j ds \tag{9c}$$

with $\mathcal{M}_i = \{j \in \{1,\dots,N\} \mid \Delta_{i0j} \neq \emptyset, j \neq i\}$. Similar considerations hold true for $\frac{\partial H_{\text{vis}}(\boldsymbol{P})}{\partial y_i}$ and are omitted.

Without the moving boundaries to invisible areas Δ_{i0} and Δ_{i0j}, the result in (9) would be equal to (2), i.e., the well-known move to centroid behavior. The additional terms can be interpreted as movement vectors that lead to revelation of invisible areas, depending on the choice of D. Higher values of D result in a higher weighting of the additional terms compared to the movement towards the center of mass of the VLVC. Low values of D or disregarding the invisible area, i.e., $D = 0$, would actually lead to robots actively reducing visible area to minimize H_{vis}. This can be explained with the sign of the integrand changing dependent on $\|\boldsymbol{q}-\boldsymbol{p}_i\|^2 > D^2$ or $\|\boldsymbol{q}-\boldsymbol{p}_i\|^2 < D^2$, turning the direction of the normal vectors $\boldsymbol{n}_i$.

Unfortunately, (9b) and (9c) require a high effort to compute, lead to unwanted movements towards the boundary of $\mathcal{Q}$ in several cases and have negligible effect in many other situations. Therefore we propose the following

Assumption 1 (Approximation of the gradient): The integral terms arising from the boundaries to invisible regions in $\frac{\partial H_{\text{vis}}(\boldsymbol{P})}{\partial \boldsymbol{p}_i}$ have negligible effect on the desired coverage behavior and the gradient can be approximated by

$$\frac{\partial H_{\text{vis}}(\boldsymbol{P})}{\partial \boldsymbol{p}_i} \approx \partial H_{\text{approx},i} = \int_{\mathcal{V}^\star_{\delta,i}} \frac{\partial}{\partial \boldsymbol{p}_i}\|\boldsymbol{q}-\boldsymbol{p}_i\|^2\phi(\boldsymbol{q})d\boldsymbol{q}. \tag{10}$$

Depending on the situation this assumption can be quite strong or very reasonable. We deliberately accept the fact that there will be no active movement towards (uncovering of) invisible areas. Further effects will be discussed in the later sections.

Using (10), the resulting control law of our approximated coverage strategy is

$$\dot{\boldsymbol{p}}_i = \boldsymbol{u}_i = k(\boldsymbol{c}_i^\star - \boldsymbol{p}_i) \tag{11}$$

with the centroid of the VLVC

$$\boldsymbol{c}_i^\star = \frac{\int_{\mathcal{V}^\star_{\delta,i}} \boldsymbol{q}\phi(\boldsymbol{q})d\boldsymbol{q}}{\int_{\mathcal{V}^\star_{\delta,i}} \phi(\boldsymbol{q})d\boldsymbol{q}}. \tag{12}$$

$H_{\text{vis}}(\boldsymbol{P})$ is no longer minimized exactly but approximately, meaning that $\frac{\partial H_{\text{vis}}(\boldsymbol{P})}{\partial \boldsymbol{p}_i} \approx 0$ in equilibrium points where $\boldsymbol{p}_i = \boldsymbol{c}_i^\star$.

As mentioned in Remark 1, there are certain points where $H_{\text{vis}}(\boldsymbol{P})$ is not differentiable, i.e., $\frac{\partial H_{\text{vis}}(\boldsymbol{P})}{\partial \boldsymbol{p}_i}$ is not defined in these points. However, our approximated gradient $\partial H_{\text{approx},i}$ exists for all $\boldsymbol{p}_i \in \mathcal{Q}_\delta$. Hence, we do not have to rely on the computation of a generalized gradient, as was done in [19] and [21].

D. Trajectories

In this subsection we provide a statement about the trajectories of the proposed system and some comments on convergence.

Theorem 1 (Trajectories in nonconvex environments): For a nonconvex polygonal environment $\mathcal{Q}$ and an arbitrary small $\delta > 0$, continuous application of (11) results in trajectories of the configuration $\boldsymbol{P}$ that never leave the invariant set $\mathcal{Q}_\delta$.

Proof: First, pointing out the fact that in convex locations the centroid of $\mathcal{V}^\star_{\delta,i}$ always lies in $\text{int}(\mathcal{V}^\star_{\delta,i})$ yields the conclusion that collisions with $\mathcal{Q}_\delta$ can only occur in concave locations. Second, applying the δ-contraction to $\mathcal{Q}$ turns all concave vertices in $\partial\mathcal{Q}$ into continuously differentiable concave circular segments in $\partial\mathcal{Q}_\delta$. Approaching concave locations $\boldsymbol{q}$ on the boundary $\partial\mathcal{Q}_\delta$, the boundary of the visibility-limited Voronoi cell $\mathcal{V}^\star_{\delta,i}$ facing $\boldsymbol{q}$ approaches the tangent in $\boldsymbol{q}$ and the centroid inevitably approaches $\text{int}(\mathcal{V}^\star_{\delta,i}) \subset \mathcal{Q}_\delta$. Hence, no trajectory exists that leaves $\mathcal{Q}_\delta$. ■

The process of approaching a concave location is illustrated in Fig. 3 in a scene with constant density. The circle symbolizes the robot position and the red cross indicates the centroid of the VLVC. After reaching an unstable equilibrium in Fig. 3b, i.e., a point where the gradient is theoretically zero, the robot moves to a stable location on either side of the symmetrical scene, due to numerical inaccuracies. In this context, another advantage of the δ-contraction becomes clear: It offers guaranteed collision avoidance with the environment by setting δ to the physical radius of the robots.

Even though convergence to a stable centroidal configuration seems obvious, since all robots move towards the centroids of their respective cells, a formal proof is still missing.

E. Limited Sensing Range

In a realistic setting, alongside the attenuation of sensing abilities through obstacles, sensors usually have a limited sensing range r, i.e., measurements beyond r are not accurate enough or yield no results at all. This kind of approach is related to the *mixed distortion-area problem* in [22], now combined with our modifications from Sections III-A and

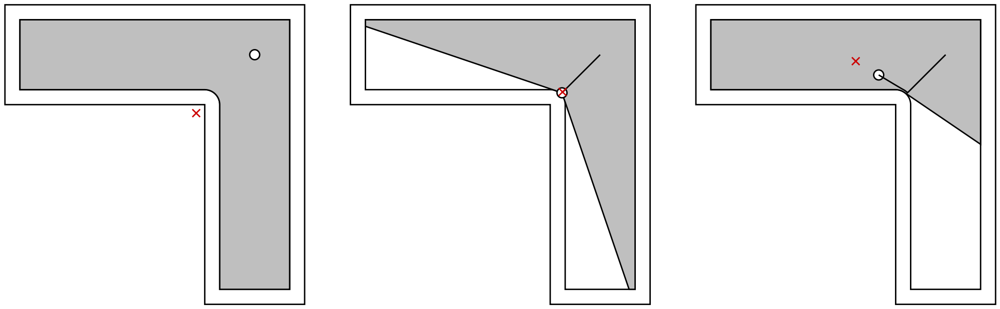

(a) Initial configuration (b) Unstable equilibrium (c) Moving to final location

Fig. 3: Approaching a concave location

III-B. The objective function for range limited coverage on visibility sets is

$$H_{\text{vis},r}(\boldsymbol{P}) = \sum_{i=1}^{N} \int_{\mathcal{V}^{\star r}_{\delta,i}} \|\boldsymbol{q}-\boldsymbol{p}_i\|^2 \phi(\boldsymbol{q}) d\boldsymbol{q} + \int_{\mathcal{Q}^{r}_{\delta,0}} r^2 \phi(\boldsymbol{q}) d\boldsymbol{q}, \tag{13}$$

with the r-limited visibility sets $\mathcal{V}^{\star r}_{\delta,i} = \{\boldsymbol{q} \in \mathcal{V}^{\star}_{\delta,i} \mid \|\boldsymbol{q} - \boldsymbol{p}_i\|^2 \leq r\}$ and the uncovered area $\mathcal{Q}^{r}_{\delta,0} = \mathcal{Q}_\delta \setminus \cup_{i=1}^{N} \mathcal{V}^{\star r}_{\delta,i}$. This definition of $H_{\text{vis},r}$ has the convenient property that all additional boundary terms that lie on distance r to a robot position are canceled out in the gradient $\frac{\partial H_{\text{vis},r}(\boldsymbol{P})}{\partial \boldsymbol{p}_i}$. Hence, the remaining gradient is similar to (9) and we can use the same assumption as in Section III-C to obtain the control law

$$\dot{\boldsymbol{p}}_i = \boldsymbol{u}_i = k(\boldsymbol{c}^{\star r}_i - \boldsymbol{p}_i). \tag{14}$$

Similar to the unlimited case, (14) moves the robots to the centroids of their respective visibility sets, herein limited by radius r. Theorem 1 from Section III-D can be applied analogously.

An additional advantage of this range limited setting is a reduced requirement on the communication range. If robots have distance $\|\boldsymbol{p}_i - \boldsymbol{p}_j\| > 2r$, the visibility sets do not intersect and there is no reason to communicate. Instead, in a worst-case scenario with unlimited sensing range, the communication range necessary is the diameter of the complete environment.

IV. RESULTS

A. Simulations

In this section we demonstrate the effectiveness of our approach in a variety of simulated environments. The δ-contraction has been applied to all scenarios with a value of $\delta = 0.15$. Figures of scene A, B and C always illustrate the final, converged sensor positions and the trajectories leading to these positions. As a first example, Fig. 4 and 5 show the comparison of a similar convex and nonconvex environment of size 6×4 with the same starting configuration of 5 sensors in the top left corner, both cases with a uniform density $\phi(\boldsymbol{q}) = 1$. In addition, Fig. 6 shows the progression of H_{vis} corresponding to the trajectories in Fig. 5. Apparently, H_{vis} is minimized despite our approximation.

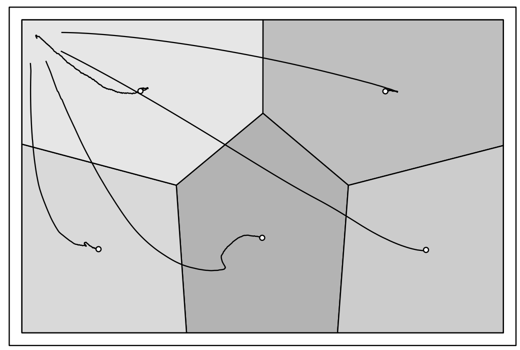

Fig. 4: Convex scene A with five sensors

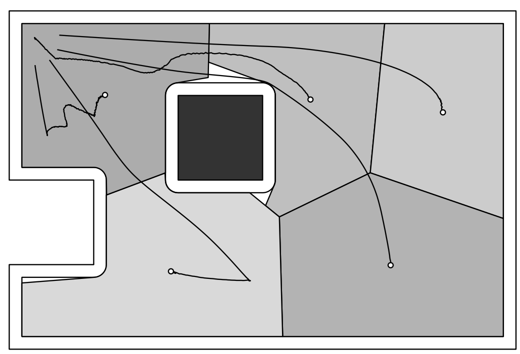

Fig. 5: Nonconvex scene A with five sensors

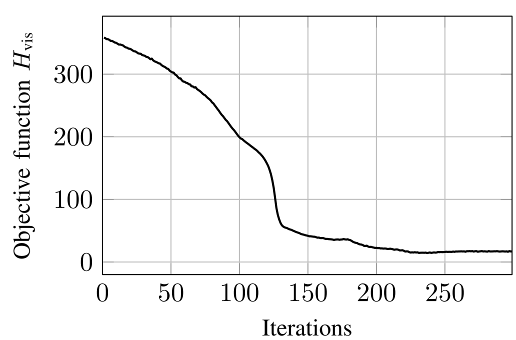

Fig. 6: Progression of H_{vis} corresponding to Fig. 5

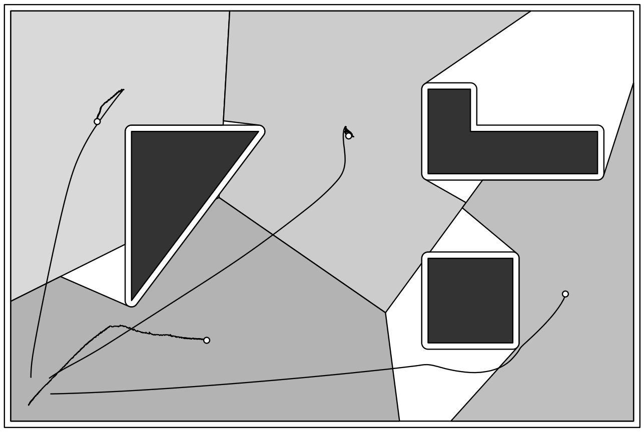

Fig. 7: Nonconvex scene B with four sensors

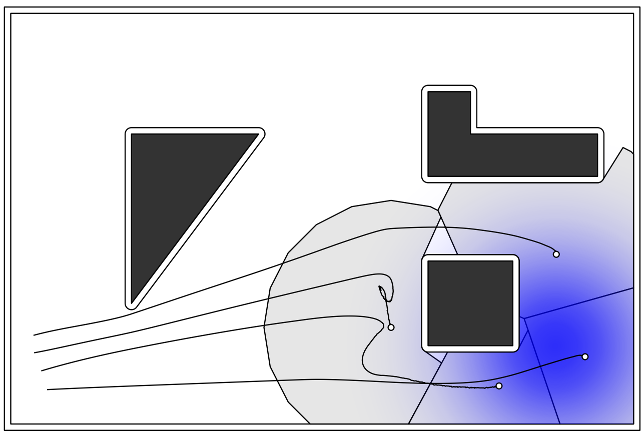

Fig. 8: Nonconvex scene B with limited sensing range and a nonuniform density

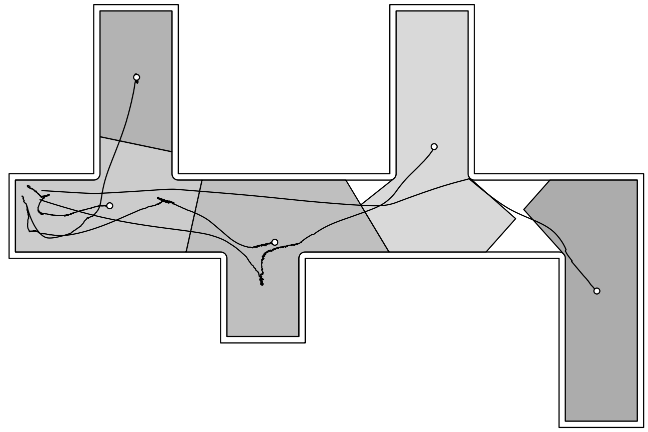

Fig. 9: Nonconvex scene C with five sensors

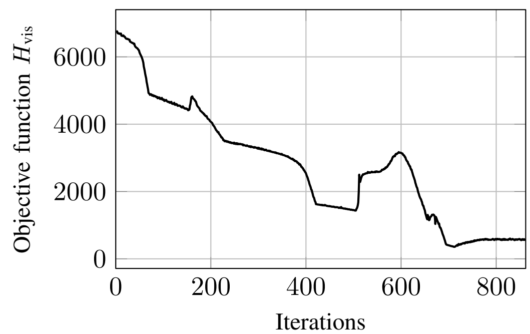

Fig. 10: Progression of H_{vis} corresponding to Fig. 9

Fig. 7 shows a coverage scenario with several obstacles in a 15×10 rectangular domain. The same environment, modified with a Gaussian density function shown in blue, is covered by agents with a limited sensing range of $r = 3$ in Fig. 8. The Gaussian function has a variance of $\sigma_x^2 = \sigma_y^2 = 4$ in both x- and y-direction with peak height 0.5 located in the bottom right part of the environment.

A corridor-like region with constant density is considered in Fig. 9, where sensors start in the far left part of the domain and spread out all the way up to the right. The progression of H_{vis} in Fig. 10 shows that our approximated gradient $\partial H_{\text{approx},i}$ does not strictly minimize the original objective. Nevertheless a good final configuration can be achieved.

In all our simulations, there was no situation where positions did not converge to a stable centroidal configuration.

B. Discussion

As a final assessment, the properties of our nonconvex Voronoi coverage will be discussed and compared with regard to optimality, computational effort and communication load. Computational effort and communication load are important factors in a distributed environment, as evaluation is done on the individual sensors, where both computation as well as communication capabilities are limited.

One important point is the choice of partition. The computation of the VLVC proposed in Section III-A is a simple intersection operation, whereas other authors have to rely on a discretization of the environment combined with a flooding method (e.g., [20]) for cell computation. Marier et al. [21] use the same partition as presented in [20]. Another additional effort is the treatment of disconnected cells, which do not arise in our case. The partition also has an influence on the required communication: Using the VLVCs, the sensors only have to communicate their position to Voronoi neighbors. Propagation of the visibility boundaries is not necessary in our case, as opposed to the compared approaches. The gain in optimality choosing the more complex partition remains uncertain. Using the simplified notion of the visibility-limited Voronoi diagram compared to [20] and [21] does not mean agents do not see the area or can not sense there, but we only disregard it in the computation of the control law.

The computation of the control input (11) is as simple as in the original approach from [1] in known environments. In unknown environments, the δ-contraction has to be computed online, but this case is rarely considered in coverage literature. In [20], an additional path planning and projection procedure is necessary at all times. Calculating the control from [21] is even more costly, due to integrals over the moving visibility frontiers and use of a generalized gradient. Further, the parameter D has to be chosen and

TABLE I: Comparison of visibility-based Voronoi coverage

	Lu et al. [20]	Marier et al. [21]	This paper
Optimality	o	$+$	o
Computat. effort	o	$-$	$+$
Communic. load	$-$	$-$	$+$

adapted appropriately to the size of the environment.

Regarding optimality, reconsider the example in Fig. 3. Optimizing H_{vis} exactly would always lead to convergence to a minimum close to the position shown in Fig. 3b (provided an appropriate choice of D), with trajectories possibly leaving $\mathcal{Q}_\delta$ temporarily. Using $\partial H_{\text{approx},i}$ leads to an unstable equilibrium and 2 stable local minima, one of which is shown in Fig. 3c. This is a case where the approximated solution can be relatively far away from the exact, in many other situations the exact and approximated minimum locations are closer together. Generally speaking, in scenes with high nonconvexity and a low number of robots, the optimality is reduced. On the other hand, especially in the case of limited sensing range frontiers to invisible regions have a low impact and the approximated solution is advantageous. Furthermore, the optimization itself is nonconvex in all nontrivial cases, even for convex environments, i.e., the configuration converges only to a local minimum with a gradient method. Still, the exact method from [21] has the advantage with respect to optimality. The results of the discussion are summarized in Table I, showing a comparison to the two closely related approaches.

V. CONCLUSIONS

We successfully transferred Voronoi coverage to nonconvex environments, proposing an approximating solution that has advantageous properties with regard to communication and computation requirements and obstacle avoidance behavior. An extended comparison of approximated solutions with the exact solutions to the objective function could lead to more interesting insights into the properties of our method. Future work could also include a more detailed look into different kinds of partitions on visibility sets and, as already mentioned, a formal proof of convergence is also open for future research.

REFERENCES

[1] J. Cortés, S. Martínez, T. Karataş, and F. Bullo, "Coverage control for mobile sensing networks," *IEEE Transactions on Robotics and Automation*, vol. 20, no. 2, pp. 243–255, 2004.

[2] S. Martínez, J. Cortés, and F. Bullo, "Motion coordination with distributed information," *IEEE Control Systems*, vol. 27, no. 4, pp. 75–88, 2007.

[3] S. Lloyd, "Least squares quantization in pcm," *IEEE Transactions on Information Theory*, vol. 28, no. 2, pp. 129–137, 1982.

[4] A. Okabe and A. Suzuki, "Locational optimization problems solved through voronoi diagrams," *European Journal of Operational Research*, vol. 98, no. 3, pp. 445 – 456, 1997.

[5] J. Cortés, S. Martínez, and F. Bullo, "Spatially-distributed coverage optimization and control with limited-range interactions," *ESAIM: Control, Optimisation and Calculus of Variations*, vol. 11, pp. 691–719, 10 2005.

[6] K. Laventall and J. Cortés, "Coverage control by multi-robot networks with limited-range anisotropic sensory," *International Journal of Control*, vol. 82, no. 6, pp. 1113–1121, 2009.

[7] M. Schwager, J. Mclurkin, and D. Rus, "Distributed coverage control with sensory feedback for networked robots," in *Proceedings of Robotics: Science and Systems*, 2006.

[8] L. C. Pimenta, M. Schwager, Q. Lindsey, V. Kumar, D. Rus, R. C. Mesquita, and G. A. Pereira, "Simultaneous coverage and tracking (scat) of moving targets with robot networks," in *Algorithmic Foundation of Robotics VIII*, ser. Springer Tracts in Advanced Robotics, G. S. Chirikjian, H. Choset, M. Morales, and T. Murphey, Eds. Springer Berlin Heidelberg, 2009, vol. 57, pp. 85–99.

[9] D. Haumann, V. Willert, and K. D. Listmann, "DisCoverage: From coverage to distributed multi-robot exploration," in *4th IFAC Workshop on Distributed Estimation and Control in Networked Systems*, Koblenz, Germany, 2013.

[10] A. Breitenmoser, M. Schwager, J.-C. Metzger, R. Siegwart, and D. Rus, "Voronoi coverage of non-convex environments with a group of networked robots," in *Proceedings of the IEEE International Conference on Robotics and Automation*, 2010, pp. 4982–4989.

[11] L. C. A. Pimenta, V. Kumar, R. Mesquita, and G. A. S. Pereira, "Sensing and coverage for a network of heterogeneous robots," in *47th IEEE Conference on Decision and Control*, 2008, pp. 3947–3952.

[12] C. Caicedo-Núñez and M. Žefran, "Performing coverage on nonconvex domains," in *IEEE International Conference on Control Applications*, 2008, pp. 1019–1024.

[13] ——, "A coverage algorithm for a class of non-convex regions," in *47th IEEE Conference on Decision and Control*, 2008, pp. 4244–4249.

[14] A. Renzaglia and A. Martinelli, "Distributed coverage control for a multi-robot team in a non-convex environment," in *IEEE IROS09 3rd Workshop on Planning, Perception and Navigation for Intelligent Vehicles*, St. Louis, États-Unis, 2009.

[15] A. Howard, M. J. Matarić, and G. S. Sukhatme, "Mobile sensor network deployment using potential fields: A distributed, scalable solution to the area coverage problem," in *Distributed Autonomous Robotic Systems 5*, H. Asama, T. Arai, T. Fukuda, and T. Hasegawa, Eds. Springer Japan, 2002, pp. 299–308.

[16] J. W. Durham, R. Carli, P. Frasca, and F. Bullo, "Discrete partitioning and coverage control for gossiping robots," *IEEE Transactions on Robotics*, vol. 28, pp. 364–378, 2012.

[17] A. Ganguli, J. Cortés, and F. Bullo, "Distributed coverage of nonconvex environments," in *Networked Sensing Information and Control*, V. Saligrama, Ed. Springer US, 2008, pp. 289–305.

[18] K. J. Obermeyer, A. Ganguli, and F. Bullo, "Multi-agent deployment for visibility coverage in polygonal environments with holes," *International Journal of Robust and Nonlinear Control*, vol. 21, no. 12, pp. 1467–1492, 2011.

[19] M. Zhong and C. G. Cassandras, "Distributed coverage control in sensor network environments with polygonal obstacles," in *17th IFAC World Congress*, 2008.

[20] L. Lu, Y.-K. Choi, and W. Wang, "Visibility-based coverage of mobile sensors in non-convex domains," in *Eighth International Symposium on Voronoi Diagrams in Science and Engineering (ISVD)*, 2011, pp. 105–111.

[21] J.-S. Marier, C.-A. Rabbath, and N. Léchevin, "Visibility-limited coverage control using nonsmooth optimization," in *Proceedings of the American Control Conference (ACC)*, 2012, pp. 6029–6034.

[22] F. Bullo, J. Cortés, and S. Martínez, *Distributed Control of Robotic Networks*. Princeton University Press, 2009.

[23] T. Lozano-Pérez and M. A. Wesley, "An algorithm for planning collision-free paths among polyhedral obstacles," *Communications of the ACM*, vol. 22, no. 10, pp. 560–570, Oct. 1979.

[24] H. Flanders, "Differentiation under the integral sign," *The American Mathematical Monthly*, vol. 80, no. 6, pp. 615–627, 1973.